Magnetic tweezers based force spectroscopy studies of the structure and dynamics of nucleosomes and chromatin

Kruithof, M.C.

CHAPTER 2

Sub-Piconewton Dynamic Force Spectroscopy Using Magnetic Tweezers[1]

Abstract

We introduce a simple method for dynamic force spectroscopy with magnetic tweezers. This method allows application of sub-piconewton force and twist control, by calibration of the applied force from the height of the magnets. Initial dynamic force spectroscopy experiments on DNA molecules revealed a large hysteresis that is caused by viscous drag on the magnetic bead and which will conceal weak interactions. Using smaller beads this hysteresis is sufficiently reduced to reveal intra-molecular interactions at sub-piconewton forces. Compared to typical quasi-static force spectroscopy a significant reduction of measurement time is achieved, allowing the real time study of transient structures and reaction intermediates. As a proof of principle nucleosome-nucleosome interactions on a sub-saturated chromatin fiber were analyzed.

[1]This chapter is based on the article: *Sub-piconewton Dynamic Force Spectroscopy Using Magnetic Tweezers* M. Kruithof, F. Chien, M. de Jager and J. van Noort, Biophysical Journal, 94 (6) 2343 - 2348

2.1 Introduction

To probe the mechanics of biomolecules at the single molecule level a variety of force spectroscopy techniques have been developed. This includes Optical Tweezers (OT), Magnetic Tweezers (MT), and Atomic Force Microscopy (AFM) [1]. With these techniques the energy landscape of biological bonds can generally be resolved accurately by applying an increasing force on a molecule and measuring its extension in time. Evans and Ritchie showed that careful analysis of the rupture force as a function of the force loading rate reveals both the interaction distance and the energy barrier of a molecular bond [2]. The energy dissipated by the rupture can be quantified from the hysteresis in a Force-Distance (F-D) cycle. For such dynamic force spectroscopy experiments OT and AFM are well suited as they both combine a position trap with nanometer resolution manipulation. However, the high spring constants of these traps in combination with the Brownian fluctuations limit the force accuracy of these techniques to approximately 1 pN for OT and 10 pN for AFM.

In contrast, MT, comprising a pair of permanent magnets in combination with a paramagnetic bead can be characterized as force clamps as they do not fix the position of the trapped bead but the applied force. The effective stiffness of the trap depends on the compliance of the polymer that tethers the bead to the surface. The applied force is calculated from the Brownian motion of the bead using equipartition theory. As a consequence of the high compliance of the tether, forces down to 10 fN are experimentally accessible, as shown by Strick et al. for example [3]. MT also clamp and constrain the rotation of the bead, giving a unique handle on DNA topology, for example. These features have made MT an indispensable tool to reveal many of the mechanical properties of DNA and DNA interacting proteins like topoisomerases, helicases, and chromatin remodellers [4]. Unfortunately, as a consequence of the small effective spring constant of these molecules at small forces and the large viscous damping of the bead, accurate quantification of the Brownian motion is time consuming and extends up to tens of minutes per force point. As a consequence, MT can typically only be operated in quasi-static force mode, where a series of force points needs to be acquired to obtain a full F-D profile [5].

In this paper we introduce dynamic force spectroscopy for MT. Here the magnetic force is calibrated to the magnet position. From this relation the applied force is calculated while the bead position is detected in real-time. A major advantage of dynamic force spectroscopy using MT compared to OT and AFM is that a sub-pN range of forces become accessible which are relevant in many biological applications. Moreover, measurement times are reduced by two orders of magnitude compared to traditional quasi-static force spectroscopy. This strong reduction of measurement time significantly relieves instrumentation drift issues commonly associated with MT experiments. Transient interactions that readily dissociate upon extended periods of increased force can now be measured with the highest accuracy. The artifacts that

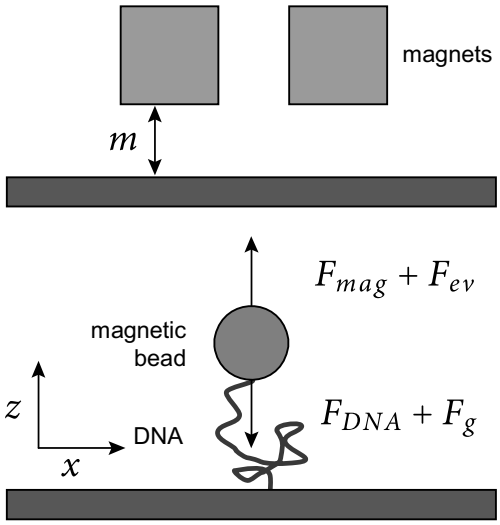

Figure 2.1: *Schematic layout of the experimental geometry. The forces pulling the bead up are the magnetic force, F_{mag}, and the force resulting from excluded volume effects, F_{ev}. The gravitational force, F_g, and the force applied by the DNA, F_{DNA}, pull the bead downwards. The dimension of the drawing are not to scale.*

are caused by the dominant role of Brownian motion at low forces, as well as the relatively high viscous drag on the bead, will be discussed and resolved.

2.2 Materials and Methods

Magnetic Tweezers

DNA-tethered paramagnetic beads were imaged in a home built inverted microscope with a CCD camera (Pulnix TM-6710CL) at 60 frames per second. The magnet position was controlled by a stepper motor-based translation stage (M-126, Physik Instrumente) with an accuracy of 200 nm. The position of the beads was measured by real time image processing using LabView software (National Instruments) with an accuracy of 10 nm. A schematic layout of the experimental geometry is shown in Fig. 2.1. During a quasi-static force measurement, the force at each magnet position was calculated from the fluctuations of the bead in the transverse direction, x, parallel to the coverslip, and from the average height of the bead, z, normal to the coverslip [3]:

$$F = k_b T \frac{\langle z(t) \rangle}{\left\langle (\bar{x} - x(t))^2 \right\rangle} \tag{2.1}$$

During a dynamic force measurement the magnets were moved towards the bead and back at a constant speed resulting in a forward and backward trace, respectively. The position of the magnets was calculated from the position of the stepper motor.

Magnetic Beads

Paramagnetic tosylactivated Dynabeads (Invitrogen) were coated with anti-digoxygenin antibodies (Sigma) according to the protocol suggested by the supplier.

Sample Preparation

A clean glass coverslip was coated with a 10 µg/mL poly-d-lysine solution (Sigma). Next, it was incubated with a polyethyleneglycol (PEG) solution containing a mixture of 20% w/v mPEG-Succinimidyl Propionic Acid (SPA)-5000 and 0.2% biotin-PEG-N-Hydroxysuccinimide (NHS)-3400 (Nektar) in sterile 0.1 M $NaHCO_3$ buffer (pH 8.5) for 3 hours at room temperature. The coverslip was then mounted on a polydimethylsiloxane (PDMS) flowcell containing a 10x4x0.4 mm flow channel, and flushed with 1 mL buffer MB (10 mM HEPES pH 7.6, 100 mM KAc, 2 mM $MgAc_2$, 10 mM $NaN_3$3, and 0.1% (v/v) Tween-20 in milli-Q water). Next, 0.1 mg/mL streptavedin (Sigma) was flushed into the cell and incubated for 10 minutes. The cell was subsequently flushed with 1 mL of MB, 400 µL 2.5 ng/µL DNA in MB and incubated for 10 minutes, 1 mL MB, 1 µL magnetic beads in 400 µL MB supplemented with 0.02% (w/v) BSA (MB+) and incubated for 10 minutes and finally flushed with MB+.

DNA and Chromatin Fibers

A construct of pBlueScript SK+ with a cloned insert containing 17 5S RNA nucleosome positioning sites was digested with HindIII and NotI. The fragment containing 17 positioning elements was purified. 1300 base pair PCR fragments (template: pBluescript K+; primers: 5'-CTAAA TTGTA AGCGT TAATA TTTTG TTAAA-3' and 5'-TATCT TTATA GTCCT GTCGG GTTTC GCCAC-3') containing either digoxygenin- or biotin-modified uracils in a ratio of 1:20 to non-modified thymine were digested with Not I and HindIII, respectively. The resulting 650 bp fragments were ligated, with an excess of 10:1, to each end of the vector fragment carrying the 17 positioning elements and used without further purification. Electrophoretic

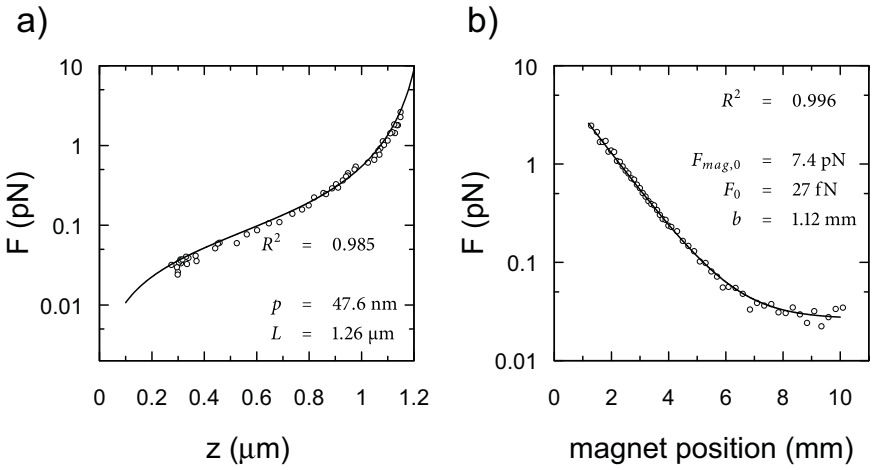

Figure 2.2: *Force calibration for dynamic force spectroscopy. (a) A F-D plot of a DNA molecule obtained with quasi-static force spectroscopy (black circles) fits the WLC model (black line). (b) The force at different magnet positions (black circles) follows an exponential decay with an additional offset (black line).*

gel analysis showed that all the vector fragments were ligated to the linker fragments. For nucleosome reconstitution, a salt dialysis with recombinant histone proteins was performed as described elsewhere [6]. The histone octamer to positioning site ratio was 1:1, but the yield of reconstitution was significantly smaller than 100%.

Atomic Force Microscopy

Sub-saturated chromatin fibers were imaged with tapping mode AFM on a Nanoscope III (Veeco) after glutaraldehyde fixation and deposition on mica.

2.3 Validation of the method

To empirically determine the relation between force and magnet position we performed quasi-static force measurements on single DNA molecules. A typical result of these measurements is shown in Fig. 2.2a. The Force-Distance plot accurately follows the Worm Like Chain (WLC) [7]:

$$F_{DNA}(z) = \frac{k_b T}{p}\left(\frac{1}{4\left(1 - z/L\right)^2} - \frac{1}{4} + \frac{z}{L}\right), \tag{2.2}$$

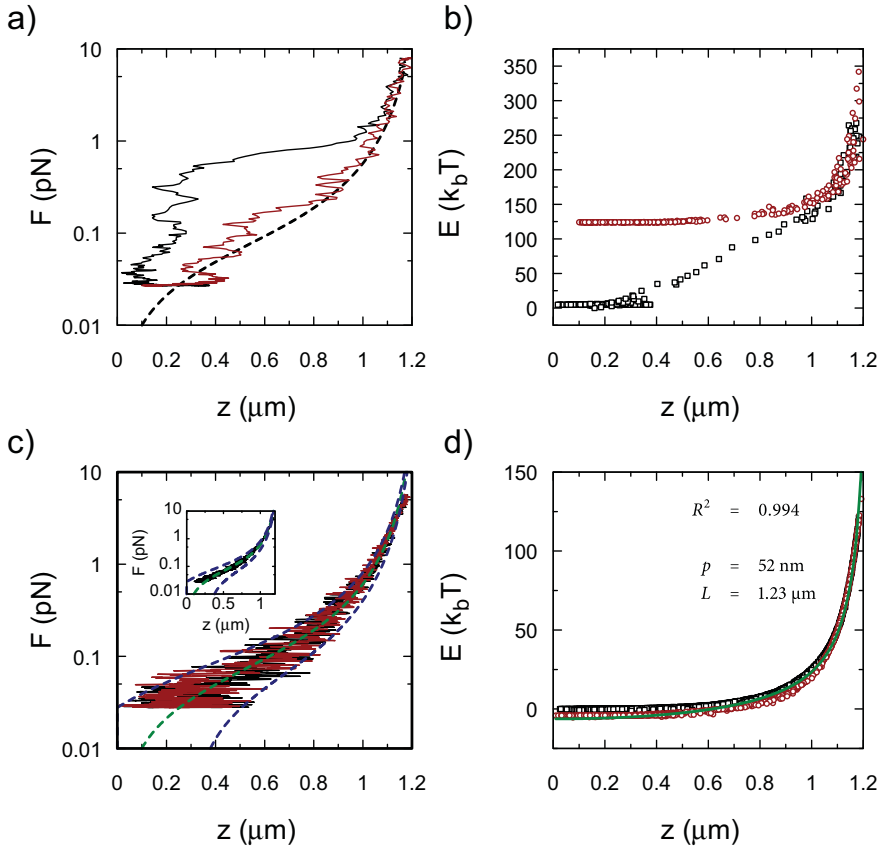

Figure 2.3: *Dynamic force spectroscopy on DNA using large and small magnetic beads. (a) Dynamic force spectroscopy using 2.8 μm beads. The forward trace (black line) and backward trace (red line) do not overlap indicating energy dissipation; the dashed black line is a WLC with a persistence length of 52 nm and a contour length of 1.2 μm. Each trace was obtained in 5 seconds. (b) The work during the experiment as a function of the extension. The forward trace (black squares) and backward trace (red circles) do not overlap, indicating dissipation. (c) Dynamic force spectroscopy using 1 μm beads. The forward trace (black line) and backward trace (red line) overlap. The dashed green line is a WLC with the persistence length and contour length taken from the fit in Fig. 2.3d. The dashed blue lines are the expected standard deviation of the Brownian noise of the bead as can be deducted from Eq. 2.2. The inset shows the average of 6 traces (black line), the noise in the traces is clearly reduced. Each trace was obtained in 5 seconds. (d) The work during the experiment as a function of the extension, the forward trace (black squares) and backward trace (red circles) overlap, indicating a fully elastic response. A WLC model was fitted to the backward trace (green line).*

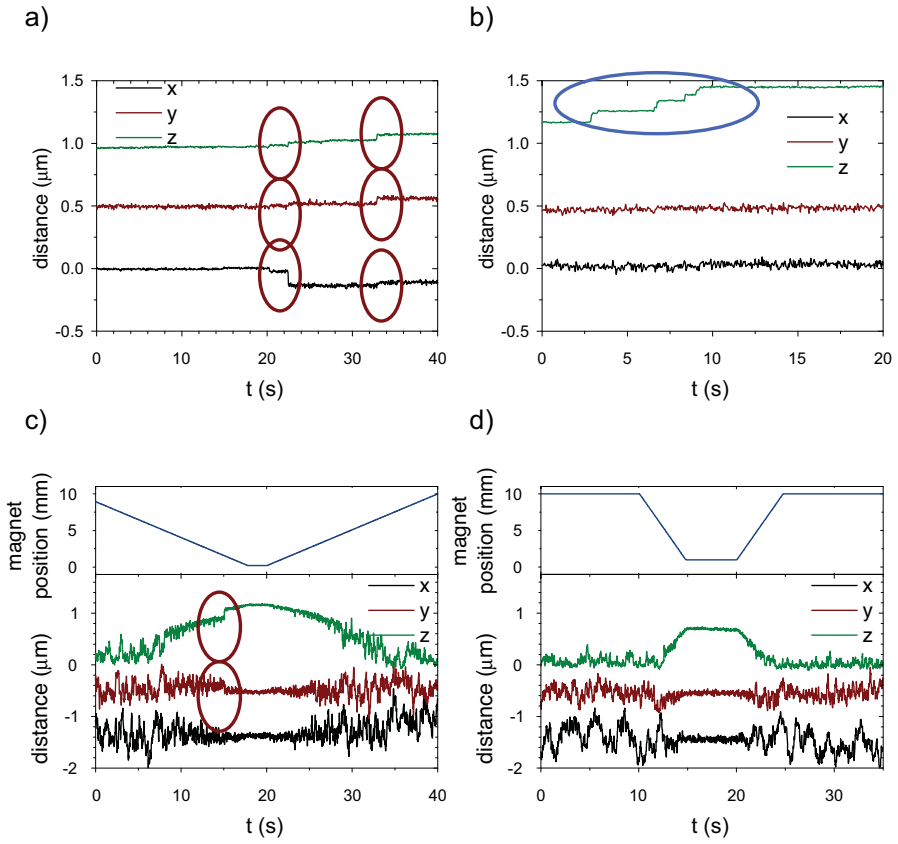

Figure 2.4: *Discrimination between disruptions of non-specific interactions with the surface and intra-molecular interactions. The time trace of a subsaturated chromatin fiber, taken at a constant force of 17 pN, shows (a) non specific surface interaction events (red circles) which were accompanied by lateral movements and (b) intra-molecular disruptions which were not accompanied by lateral movement (blue circle). (c) The time trace of a dynamic force measurement shows an instance of a rupture (red circles) which was accompanied by lateral movement. We attribute this to non-specific surface interactions. (d) The time trace of the F-D curve shown in Fig. 4b in which no lateral movement was detected.*

with thermal energy $k_b T$, extension z, fitted persistence length p = 48 nm, and contour length L = 1.26 µm. In Fig. 2.2b we plotted the obtained force as a function of the magnet position. We found that the force, F_{tot}, decays exponentially with the magnet position, according to:

$$F_{tot} = F_{mag,0} e^{-m/b} + F_0, \tag{2.3}$$

where m is the distance between the top of the fluidic cell and the magnets as depicted in Fig. 2.1. $F_{mag,0}$ is the maximal force, b the decay length of the magnetic force, and F_0 a constant offset. In our setup $F_{mag,0}$ was 18 ± 2 fN for 2.8 µm diameter beads and 6 ± 1.4 fN for 1 µm diameter beads. We found the decay length, which is defined by the geometry of the set-up, to be constant, b = 1.1 ± 0.07 mm. Below 100 fN the observed force is independent of the magnet position. In this regime excluded volume effects, pushing the bead away from the surface and gravity, pulling the bead down, dominate [8]. We estimated F_0, the sum of the force originating from gravity and from excluded volume effects to be approximately 31 fN, in good agreement with a fitted offset of 27 fN. During a dynamic force measurement Eq. 2.3 was used to calculate the force from the magnet position.

To test the dynamic force mode on a DNA molecule we acquired a F-D cycle shown in Fig. 2.3a. Each forward pulling trace was acquired in 5 seconds, the backward trace was acquired at the same speed. Note that this is much shorter than a quasi-static measurement like the one shown in Fig. 2.2a, which was measured in about an hour. Surprisingly, a significant hysteresis was observed between the forward (increasing force) and backward (decreasing force) trace. When compared to the WLC-fit obtained with quasi-static force spectroscopy it appeared that only at forces above 1 pN both the forward and the backward trace follow the WLC. At forces below 1 pN, however, only the backward trace matches the WLC curve. As DNA has been shown to deform elastically at forces below its melting transition, i.e. below 60 pN; [5], the origin of this hysteresis cannot be internal disruption of the DNA structure, and must therefore be attributed to external dissipation.

Non-specific interactions between the DNA and/or bead with the surface are commonly observed in these measurements, especially at low forces and might alternatively explain the observed behavior. Disruption events of such non-specific interactions are generally accompanied by a movement in the lateral direction, as shown in Fig. 2.4. In order to discriminate between surface interactions and intra-molecular interactions we used the absence of lateral movement as a selection criterion. Furthermore, by PEG passivation of the surface, the number of traces that showed lateral movement was reduced to a complete absence in DNA traces and a very small fraction in the case of chromatin fibers. Thus non-specific interactions between the tether and the surface can be discarded as the origin of the hysteresis.

Understanding the nature of the observed hysteresis is a requirement for F-D analysis of more

complex structures. Therefore, we considered the equation of motion of the tethered bead:

$$F_{DNA}(z) = F_{mag} - \gamma \frac{dz}{dt}, \tag{2.4}$$

with z the position of the bead and γ the drag coefficient. Inertia forces can readily be neglected. Rapid changes in magnetic force will induce an extra friction force that makes the bead lag behind. The drag coefficient γ is given by Stokes' law:

$$\gamma = 6\pi\eta r, \tag{2.5}$$

with bead radius r and viscosity η. Note that the drag coefficient at close proximity to the surface γ^* can be significantly larger than the drag coefficient given by Eq. 2.5 when the radius of the bead, r, is comparable to the distance between the bead and the coverslip, z, [9]:

$$\gamma^* = \left(1 + \frac{r}{z} + \frac{r}{6z + 2r}\right)\gamma \tag{2.6}$$

During a dynamic force measurement we assumed that the force on the molecule is equal to the applied magnetic force determined in a quasi-static measurement. However, from Eq. 2.4 it is clear that friction also contributes to the applied force, $F_{fr} = \gamma \frac{dz}{dt}$. In the case of DNA the viscous drag is mostly limited to the entropic regime where DNA behaves like a Hookian spring, $z = \frac{F_m}{k}$ with $k = \frac{3}{2}\frac{k_b T}{pL}$, therefore, using Eq. 2.3, the relative contribution of the friction, F_{fr}/F_m, can be written as:

$$\frac{F_{fr}}{F_m} = \frac{v_{mag}\gamma^*}{bk}, \tag{2.7}$$

with v_{mag} the velocity of the magnets and k the spring constant of the tether. with , resulting in the following formula for the relative contribution of the friction:

$$\frac{F_{fr}}{F_m} = \frac{2}{3}\frac{pv_{mag}L\gamma^*}{bk_b T} \tag{2.8}$$

The assumption that the force on the molecule is equal to the applied magnetic force is only valid when the friction force is negligible compared to the magnetic force ($F_{fr}/F_m \ll 1$). The maximum magnet velocity typically used in experiments was 2 mm/s. For 2.8 μm diameter beads $F_{fr}/F_m = 0.43$ which is clearly not negligible. Decreasing the bead diameter will decrease this contribution. For example the contribution of friction to the total force on 1 μm diameter beads is much smaller ($F_{fr}/F_m = 0.15$) and will lead to a more accurate F-D curve as quantified in the next paragraph. A dynamic F-D plot measured using a 1 μm diameter bead is shown in Fig. 2.3c. In contrast to the data obtained with 2.8 μm diameter beads (Fig. 2.3a), the data follow the WLC model accurately and no obvious hysteresis was observed between

the forward and the backward trace.

2.4 Energy analysis

Brownian motion of the bead causes the large fluctuations in the low force regime as demonstrated in Fig. 2.3a, making it difficult to asses any residual dissipation. Averaging of Brownian fluctuations from multiple F-D curves, reduces this effect, as shown in Fig. 2.3c, inset. However, averaging precludes the ability to resolve single ruptures that are not synchronous in repeated experiments, a major advantage of dynamic force spectroscopy. As an alternative we calculated the work done during the experiment, i.e. $E(t) = \int_0^t F(t^*)\frac{dz}{dt^*}dt^*$, which results in an Energy-Distance (E-D) plot as shown in Fig. 2.3d. As the Brownian motion is now integrated all fluctuations will collapse on the curve:

$$E(z) = \int_0^z F_{DNA}(z^*)dz^* = \frac{1}{4}\frac{k_b T z^2 (2z - 3L)}{pL(z - L)} \tag{2.9}$$

Both the forward and backward trace fit very well to Eq. 2.9 for $p = 49$ nm and $L_0 = 1.18$ µm.

From the measurements we also obtained the total dissipated energy, in a single F-D cycle, which manifests itself as hysteresis in the F-D plot. After a full F-D cycle the dissipation was around $3\,k_b T$ for $1\,\mu m$ diameter beads, compared to $130\,k_b T$ for measurements with $2.8\,\mu m$ diameter beads. Alternatively, an increase of the measurement time for each trace, from 5 to 60 seconds, decreased the hysteresis on a $2.8\,\mu m$ bead (data not shown) and resulted in a dissipation of $6\,k_b T$. These values are in close agreement with numerical solutions of Eq. 2.4, 5 and 6, for DNA with a contour length of $1.2\,\mu m$, a persistence length of 52 nm and a measurement time corresponding to 5 seconds. For a dynamic F-D experiment these calculations resulted in a dissipation of $147\,k_b T$ for $2.8\,\mu m$ diameter beads and $3\,k_b T$ for $1\,\mu m$ diameter beads.

From these experiments we can conclude that using smaller magnetic beads i) dissipation from viscous drag was negligible i.e. the molecule is permanently in equilibrium with the magnetic force ii) non-specific interactions of the bead and/or DNA with the surface were negligible and iii) DNA extension is fully elastic at forces down to 10 fN.

In the current measurements the force was increased exponentially in time, effectively emphasizing the low force regime. With a more advanced, non-linear control of the magnet position one could also linearly ramp the force, making low force dynamic force spectroscopy MT experiments possible that are compatible with the framework developed for previous studies (2).

2.5 Dynamic force spectroscopy on nucleosome-nucleosome interactions

In eukaryotes DNA is condensed into chromatin. Whereas the structure of the nucleosome, the first step in DNA condensation, is known with atomic precision [10], higher order structures remain highly elusive [11]. Full understanding of higher order structure and dynamics will require detailed knowledge of all interactions between the nucleosomes. However, only rough estimates of the interaction energy are currently available due to a lack in force accuracy and the common use of chromatin reconstituted from highly heterogeneous cell extracts [12]. We recently obtained well-defined, fully saturated chromatin fibers that adopt a 30 nm fiber structure [13]. These extremely well ordered structures are stabilized by multiple nucleosome-nucleosome interactions that act in concert. Such 30 nm fibers, when measured using dynamic force spectroscopy as described in this paper, resist forces up to 4.5 pN, after which the structure unfolds cooperatively. Due to the cooperative nature of unfolding, individual interactions between nucleosomes were completely obscured in these experiments (see chapter 4 of this thesis). To resolve individual nucleosome-nucleosome interactions we performed dynamic force spectroscopy on individual sub-saturated chromatin fibers in which nucleosomes can interact but are too sparse to adapt highly condensed structures.

AFM imaging of the sub-saturated chromatin fibers reveals a large variation of the number and position of nucleosomes on each DNA template molecule, with an average number of nucleosomes per molecule of 4 ± 3, as shown in Fig. 2.5a. Some of the nucleosomes interact, causing looping of the DNA as indicated by the arrow. In Fig. 2.5b and c, F-D and E-D plots of a measurement on a single sub-saturated chromatin fiber are shown. Compared to bare DNA, Fig. 2.3c, the tether extension is significantly reduced. At an applied force of around 0.5 pN the structure ruptured to an extended length, after which the forward and backward traces overlap. In the E-D plot, we observed a total energy dissipation of 20 $k_b T$ that we attributed to the rupture of nucleosome-nucleosome interactions. The dissipated energy varied significantly between F-D cycles pointing at different interactions in each refolding cycle.

After rupture of the interactions between nucleosomes the DNA is expected to follow the WLC model, having a reduced contour length because of DNA wrapping in nucleosomes and a reduced apparent persistence length as a result of the sharp bends at the entry and exit sites of a nucleosome [14]. Indeed the backward trace in Fig. 2.5c fits well to Eq. 2.9, with $L = 0.89\,\mu\text{m}$ and $p = 18\,\text{nm}$. It is clear that since these two effects are correlated, a smaller contour length indicates more nucleosomes resulting in a smaller apparent persistence length. From the amount of wrapped DNA, 310 nm, it follows that this fiber contained 6 nucleosomes. The results ob-

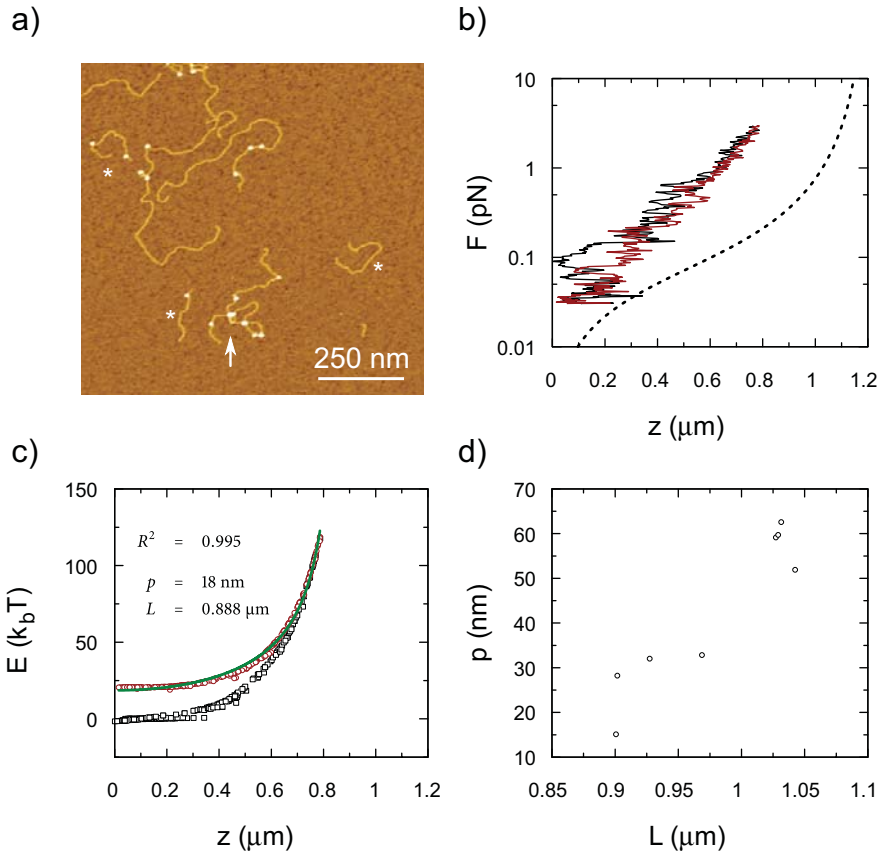

Figure 2.5: *Dynamic force spectroscopy on sub-saturated chromatin fibers (a) AFM image of the used chromatin fibers. Possible nucleosome-nucleosome interactions are indicated by an arrow. Stars denote PCR fragments used in the MT for linking the fiber to the bead and the surface. (b) Dynamic force spectroscopy on these chromatin fibers. The forward trace (black line) and backward trace (red line) do not overlap at forces smaller than 1 pN. The dashed black line is a WLC with a persistence length of 52 nm and a contour length of 1.2 µm, appropriate for a bare DNA tether. Each trace was obtained in 5 seconds. (c) The work during the experiment as a function of the extension. The forward trace (black squares) and backward trace (red circles) do not overlap and show an offset that can be attributed to disruption of nucleosome-nucleosome contacts. The backward trace (red circles) closely follows the WLC model (green line). (d) The fitted contour length of different sub-saturated chromatin fibers plotted versus the fitted persistence length.*

tained for several molecules were further analyzed, Fig.2.5d. As expected, a clear correlation between the resulting contour length and apparent persistence length was observed. For a quantitative comparison of these traces we divided the traces into two populations, the first with a contour length larger than 1 μm, containing very few or no nucleosomes, and the second with a contour length smaller than 1 μm, containing more than 4 nucleosomes. We averaged the apparent persistence length, contour length and dissipated energy over the traces within each population. The apparent persistence length differed significantly between the two populations 27 ± 8 nm and 58 ± 5 nm, respectively. The average dissipated energy was higher for the population with the smaller contour length ($16 \pm 8\ k_b T$ versus $10 \pm 6\ k_b T$). However the variations in dissipated energy are large especially in the case with the larger amount of nucleosomes. This can be expected because these unstructured arrays can adopt different nucleosome-nucleosome interactions in each F-D cycle.

Recently, Mihardja et al. reported the unwrapping of DNA within a single nucleosome at forces between 2 and 4 pN [15]. At comparable pulling rates we did not observe any unwrapping of the DNA from the nucleosomes up to forces of 6 pN. When the magnets were positioned to apply a maximum force for an extended period of time we did observe unwrapping, as plotted in Fig. 2.4c, showing that we can use dynamic force spectroscopy to study transient structures that have a limited lifetime under an applied load.

2.6 Conclusion

In conclusion, we developed a method for fast real-time sub-piconewton dynamic force spectroscopy using magnetic tweezers. We showed that the energy dissipation due to viscous drag is dependent on bead diameter. The large Brownian fluctuations of the bead position that occur at low forces conveniently collapse on a well-defined energy-distance plot, allowing accurate analysis of dynamic force spectroscopy data and calculation of the dissipated energy. As a proof of principle, measurements on single sub-saturated chromatin fibers revealed a clear correlation between contour length and apparent persistence length. Nucleosome-nucleosome interactions that rupture at 0.5 pN with a dissipated energy in the range of 10 to 16 $k_b T$ were observed.

Bibliography

[1] H. Clausen-Schaumann, M. Seitz, R. Krautbauer, and H. Gaub, "Force spectroscopy with single bio-molecules," *Current opinion in chemical biology*, vol. 4, pp. 524–30, Oct 2000.

[2] E. A. Evans and K. Ritchie, "Dynamic strength of molecular adhesion bonds.," *Biophys. J.*, vol. 72, pp. 1541–55, Apr 1997.

[3] T. R. Strick, J.-F. Allemand, D. Bensimon, A. Bensimon, and V. Croquette, "The elasticity of a single supercoiled dna molecule," *Science*, vol. 271, pp. 1835–7, Mar 1996.

[4] J. Zlatanova and S. H. Leuba, "Magnetic tweezers: a sensitive tool to study dna and chromatin at the single-molecule level," *Biochem Cell Biol*, vol. 81, pp. 151–9, Jun 2003.

[5] C. Gosse and V. Croquette, "Magnetic tweezers: micromanipulation and force measurement at the molecular level," *Biophys J*, vol. 82, pp. 3314–29, Jun 2002.

[6] C. Logie and C. L. Peterson, "Catalytic activity of the yeast swi/snf complex on reconstituted nucleosome arrays," *EMBO J*, vol. 16, pp. 6772–82, Nov 1997.

[7] C. Bustamante, J. F. Marko, E. Siggia, and S. Smith, "Entropic elasticity of lambda-phage dna," *Science*, vol. 265, pp. 1599–600, Sep 1994.

[8] D. Segall, P. C. Nelson, and R. Phillips, "Volume-exclusion effects in tethered-particle experiments: bead size matters.," *Phys. Rev. Lett.*, vol. 96, p. 088306, Apr 2006.

[9] M. Bevan and D. Prieve, "Hindered diffusion of colloidal particles very near to a wall: Revisited," *The Journal of Chemical Physics*, vol. 113, no. 3, pp. 1228–1236, 2000.

[10] K. Luger, A. W. Mäder, R. K. Richmond, D. F. Sargent, and T. J. Richmond, "Crystal structure of the nucleosome core particle at 2.8 a resolution," *Nature*, vol. 389, pp. 251–60, Sep 1997.

[11] D. J. Tremethick, "Higher-order structures of chromatin: the elusive 30 nm fiber," *Cell*, vol. 128, pp. 651–4, Feb 2007.

[12] Y. Cui and C. Bustamante, "Pulling a single chromatin fiber reveals the forces that maintain its higher-order structure.," *Proc. Natl. Acad. Sci. U.S.A.*, vol. 97, pp. 127–32, Jan 2000.

[13] V. A. T. Huynh, P. J. J. Robinson, and D. Rhodes, "A method for the in vitro reconstitution of a defined "30 nm" chromatin fibre containing stoichiometric amounts of the linker histone," *J. Mol. Biol.*, vol. 345, pp. 957–68, Feb 2005.

[14] I. M. Kulić, H. Mohrbach, V. Lobaskin, R. Thaokar, and H. Schiessel, "Apparent persistence length renormalization of bent dna.," *Physical review. E, Statistical, nonlinear, and soft matter physics*, vol. 72, p. 041905, Dec 2005.

[15] S. Mihardja, A. Spakowitz, Y. Zhang, and C. Bustamante, "Effect of force on mononucleosomal dynamics.," *Proc. Natl. Acad. Sci. U.S.A.*, vol. 103, pp. 15871–6, Oct 2006.